Relative Rate Observer Self-Tuning of Fuzzy PID Virtual Inertia Control for An Islanded microgrid

Ahmed H. Mohamed
Helwan University, Cairo, Egypt., ahmedhamada215@gmail.com

Helmy M. El Zoghby
Helwan University, Cairo, Egypt., helmy_028123288@yahoo.com

Mohiy Bahgat
Helwan University, Cairo, Egypt., drmohiybahgat@yahoo.com

A. M. Abdel Ghany
Higher Engineering Institute-Thebes Academy, Helwan University, Cairo, Egypt., ghanyghany@hotmail.com

Relative Rate Observer Self-Tuning of Fuzzy PID Virtual Inertia Control for an Islanded Microgrid

Ahmed H. Mohamed [a,*], *Helmy M. El Zoghby* [a], *Mohiy Bahgat* [a], *A. M. Abdel Ghany*[b]

[a] *Helwan University, Cairo, Egypt.*

[b] *Higher Engineering Institute-Thebes Academy, Helwan University, Cairo, Egypt.*

A B S T R A C T

Expanding the usage of renewable energy in islanded microgrids leads to a reduction in its total inertia. Low inertia microgrids have difficulties in voltage and frequency control. That affected saving its stability and preventing a blackout. To improve low inertia islanded microgrids' dynamic response and save their stability, this paper presented relative rate observer self-tuning fuzzy PID (RROSTF-PID) based on virtual inertia control (VIC) for an islanded microgrid with a high renewable energy sources (RESs) contribution. RROSTF-PID based on VIC's success in showing remarkable improvement in the microgrid's dynamic response and enhancement of its stability. Moreover, it handles different contingency conditions successfully by giving the desired frequency support. Ant colony optimization (ACO) technique is used to find the optimal values of the RROSTF-PID based on VIC parameters. Furthermore, using MATLAB TM/Simulink, RROSTF-PID based on VIC response is compared to Optimal Fuzzy PID (OF-PID) based VIC, Fuzzy PID (F-PID) based VIC, PID-based VIC, conventional VIC responses, and the microgrid without VIC response under different operation conditions.

1. Introduction

Here introduces the paper, and put a nomenclature if necessary, in a box with the same font size as the rest of the paper. The paragraphs continue from here and are only separated by headings, subheadings, images and formulae. The section headings are arranged by numbers, bold and 9.5 pt. Here follow further instructions for authors.

Nowadays, it is more interesting to use renewable energy sources (RESs). There is an expansion in using renewable energy sources. That expansion may be instead of a synchronous generator in a traditional power system. While the rotating mass in a synchronous generator supplies the inertia to the power system from its stored kinetic energy [1]. Renewable energy sources (RESs) have no present or low contribution to the system inertia due to their power electronics interfaces [2]. So, increasing the penetration of RESs in the power system can lead to a reduction in the total system inertia. The power system with law inertia might become an insecure system with a difficulty in saving the system voltage/frequency stability [3].

The islanded microgrids that depend on renewable energy sources (RESs) may have a problem with the dynamic stability. Increasing the contribution of the RESs makes achieving dynamic stability more difficult. Moreover, system voltage/frequency oscillation can occur because of the microgrid's low inertia [4]. If the voltage/frequency values are not within an acceptable range, the system may become unstable [5].

Dealing with difficulty in voltage and frequency control in the low inertia islanded microgrids, the concept of VIC is presented. The main idea of VIC is to emulate the response of the conventional generator that provides the system inertia. The VIC improves the stability of the system and allows more contributions from the RESs [1, 6].

The VIC is applied to power inverters and energy storage systems (ESS) to achieve the behavior of a synchronous generator (inertia and damping properties). That enhances the stability of the microgrid frequency [3-4]. Based on the rate of change of frequency (RoCoF), the VIC provides the microgrid with additional active power that improves the microgrid dynamic response [6].

Many researches on VIC aim to enhance the stability of the power system frequency. In [7] a derivative controller based on VIC is used for interconnected power systems with a high contribution of renewable sources of energy to improve the frequency stability. In [6] Proportional-integral (PI) -based VIC for an isolated microgrid with high RESs penetration to minimize the frequency deviations and enhance the stability. The concept of VIC is proposed via an extended virtual synchronous generator. That supports the frequency control and improves inertia response for a microgrid [8]. In [9], an inverter control strategy is introduced to emulate the behaviors of a synchronous generators to enhance the frequency stability for a smart grid. Moreover, a solar power system that is connected to the grid under variable temperature and irradiance has a novel adaptive VIC in [10]. In [11], hybrid AC/DC microgrid systems are supported by inertia from a virtual synchronous generator. In [12] virtual inertia control is introduced for DC microgrid integrating high proportions of renewable energy to regulate the DC bus voltage. A tidal turbine power plant improves frequency regulation by using a capacitive energy storage system to supply the system with virtual inertia in [13]. In [14] a superconducting magnetic energy storage (SMES)-based VIC system is used for maintaining good frequency stability for a microgrid with renewables.

Another researches represent the virtual inertia control (VIC) by using self-adaptive controllers to adapt to different disturbance and contingency conditions, which enhance the system stability and improve the dynamic response. A self-adaptive inertia and damping combination control of a virtual synchronous generator is proposed in [15] for frequency stability improvement for a microgrid. In [4], a fuzzy logic control technique is used to determine the constant of the virtual inertia for the frequency stability enhancement of a microgrid with a high share of RESs. Furthermore, in [16], a robust FLC is proposed for superconducting magnetic energy storage (SMES) in power systems with low inertia. However, the frequency stability still needs improvements especially in the case of islanded microgrids with high penetration of RESs, in order to enhance the microgrid stability and prevent blackouts.

Several control techniques based on VIC are presented in this paper.

       1-   Fuzzy PID (F-PID) controller (Fuzzy like PID controller).

       2-   Optimal Fuzzy PID (OF-PID) controller.

       3-   Relative rate observer (RRO) self-tuning fuzzy PID (RROSTF-PID).

These control techniques change control parameters to achieve more improvement in the system dynamic response. Fuzzy logic can deal with the system with complex behavior and is used to change control parameters to achieve system frequency stability with high RESs penetration and adapt to different contingency conditions.

The low inertia islanded microgrid response with these control techniques under various disturbances is studied using MATLABTM/Simulink software. The output result is compared with the response of the microgrid without VIC, the microgrid with conventional VIC (CVIC), and with VIC based on an optimal PID controller, with a microgrid considering domestic loads (residential and industrial), and the high contribution of wind and solar power plants.

2. System Configuration

2.1. Studied Islanded Microgrid Modeling

As shown in Fig. 1, the studied islanded microgrid is a hybrid microgrid containing conventional and renewable energy sources to feed the industrial and residential loads (domestic loads). The studied islanded microgrid consists of a 20MW non-reheat thermal power plant (as a conventional energy source), a 4MW solar power plant, and an 8MW wind power plant (as renewable energy sources), a 15MW domestic load, and an energy storage system of 5MW. The system base is 20MW [6].

The studied microgrid dynamic model is shown in Fig. 2, which includes the microgrid control area, a thermal power plant, solar and wind power plants, and domestic loads [6]. The thermal power plant model includes primary and secondary frequency controllers into consideration. The generator governor action is represented by primary frequency control [1]. The secondary frequency control is identified in the model by an integral controller. For non-reheat thermal power plants, the physical constraints are also represented by generation rate constraints (GRCs), which set the permissible output power of the unit. As well as the limitations of the turbine valve/gate (the maximum and minimum limit). The GRC is adjusted to be 20% p.u. MW/min and the valve gate limits are adjusted to be ±0.3 p.u.MW [6, 17]. Table 1 displays the dynamic parameter values of the studied islanded microgrid [6].

Table 1 - Values of the Microgrid Parameters.

Parameter	Value
Ki (s)	0.05
Tg (s)	0.1
Tt (s)	0.4
R (Hz/p.u.MW)	2.4
D (p.u.MW/Hz)	0.015
H (p.u.MW s)	0.083
TVI (s)	10
Twt (s)	1.5
Tpv (s)	1.8
KVI (s)	0.5
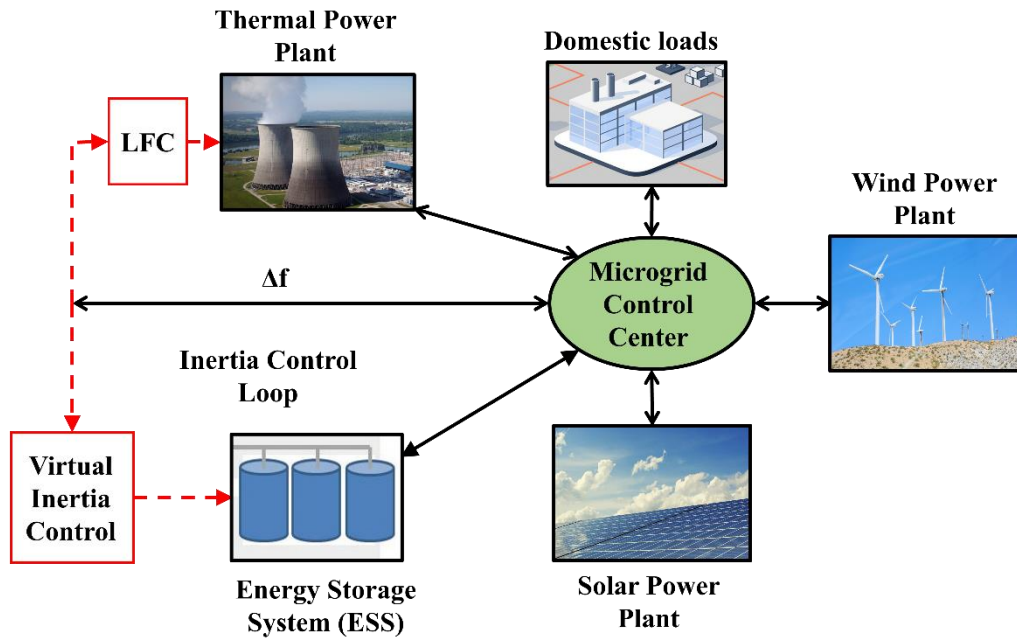
Fig. 1 - Simplified Studied Microgrid Model
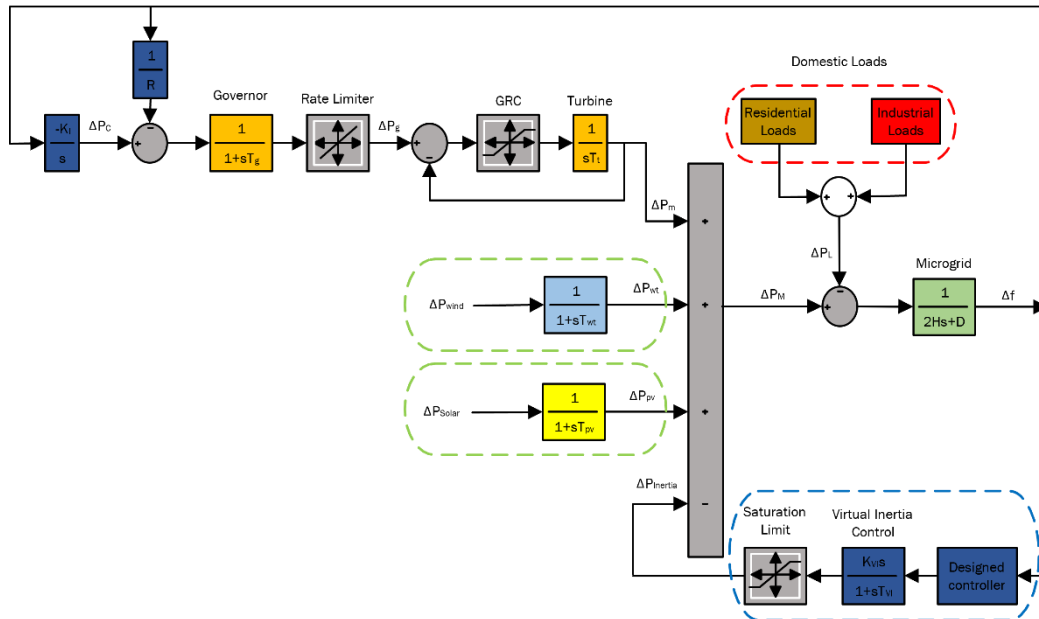
Fig. 2 - The studied islanded microgrid dynamic model.

2.2. Modeling of VIC for Studied Islanded Microgrids

By increasing the contribution of RESs to the system, the system's overall inertia is decreased. which affects the dynamic response of the system. Thus, VIC focuses on the ability to emulate the inertia and damping properties of a conventional generator, increase system inertia, and allow for more contribution of RESs to the microgrid while maintaining frequency stability.

As shown in Fig. 3, conventional VIC (CVIC) is based on a derivative controller, which is regarded as the basic controller idea that adds needed extra active power based on ROCOF determination, and a low pass filter is implemented to prevent the effect of frequency measurement noise and emulate the ESS dynamic response [3][6].

This paper aims to investigate the use of VIC based on Fuzzy PID and RROSTF-PID controllers to enhance microgrid frequency stabilization under contingency conditions such as the sudden connecting or disconnecting of a large load in the presence of RESs high contributions.
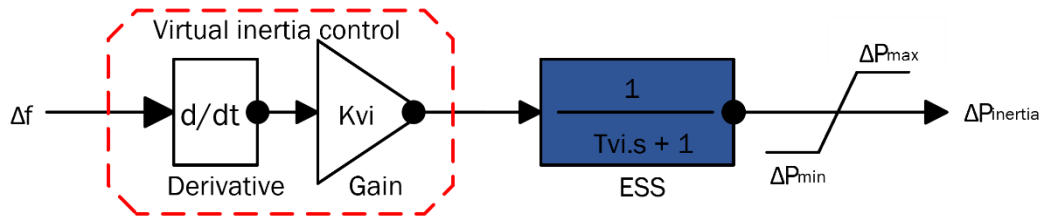
Fig. 3 - The studied islanded microgrid dynamic model.

3. Fuzzy Controller Based Virtual Inertia Control

Fuzzy logic control (FLC) main idea was introduced in [18]. In [19], Mamdani uses FLC to design controllers for ill-modeled systems. After that, FLC shows high quality in many applications [20][21]. Fuzzy PID control is used to improve the power system dynamic stability [22]. LFC of multi-area systems by using Fuzzy PID control in [23].

Fig. 4 shows the main structure of FLC. Error (e) and rate of change of error (Δe) signals (input signals) are converted into linguistic values (fuzzification). Then, Fuzzy Inference makes a decision using fuzzy rules. Finally, the center of gravity method (equ.1) is used to convert the fuzzy output to crisp output values (defuzzification) [24, 25].
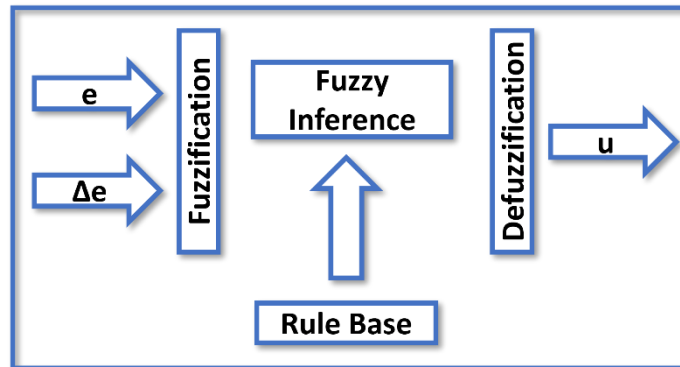
Fig. 4 - The main structure of FLC.

$$u = \frac{\sum_{k=1}^{n} u(u_k) u_k}{\sum_{k=1}^{n} u(u_k)} \tag{1}$$

Where:

$u(u_k)$: membership grad of the element u_k.

u: output of fuzzy control.

n: the number of discrete values in the universe of discourse.

Fuzzy controller output depends on the state of the system that is defined by FLC input signals (e and Δe signals) so that enhancement of the system's dynamic response [26]. The good performance of the Fuzzy controller helps to improve the system robustness.

The fuzzy controller can act like a PD controller or a PI controller and give their response. The integration between fuzzy proportional-derivative (F-PD) and fuzzy proportion-integral (F-PI) gives a Fuzzy Proportional-integral-derivative (F-PID) controller that acts like a Proportional-integral-derivative (PID) controller [27]. Fig.5 shows the Fuzzy PID controller model structure. Δf is the input signal for our system. K1 and K2 are the input gains. K3 and K4 are the output gains. FLC has two input memberships that are the same as shown in Fig. 6 and Fig. 7 shows the FLC output membership. All memberships are triangular membership functions. Table 2 shows the FLC rule base and Table 3 shows the relationship between the conventional PID controller (the transfer function is shown in equ. 2) gain parameters and the FLC gains [26, 28, 29, 30].

$$Gc\,(s) = K_p + \frac{K_i}{s} + K_d\,s \tag{2}$$

Kp: Proportional gain.

ki: Integral gain.

kd: Derivative gain.

K1 is determined as in equ. 3:

$$K1 = \frac{Fuzzy\ membership\ boundary\ values\ of\ error}{\max\ (error\ crisp\ value)} \tag{3}$$

The optimal gain parameters of the PID controller are determined by using ant colony optimization. After that, these gains are used to determine the FLC gains to act as the optimal PID controller. Table 4 shows PID and F-PID controller gain values.
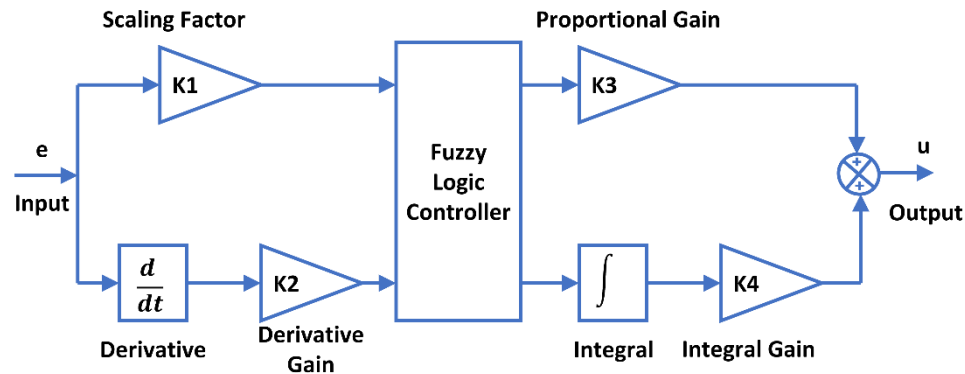
Fig. 5 - Fuzzy PID controller model.
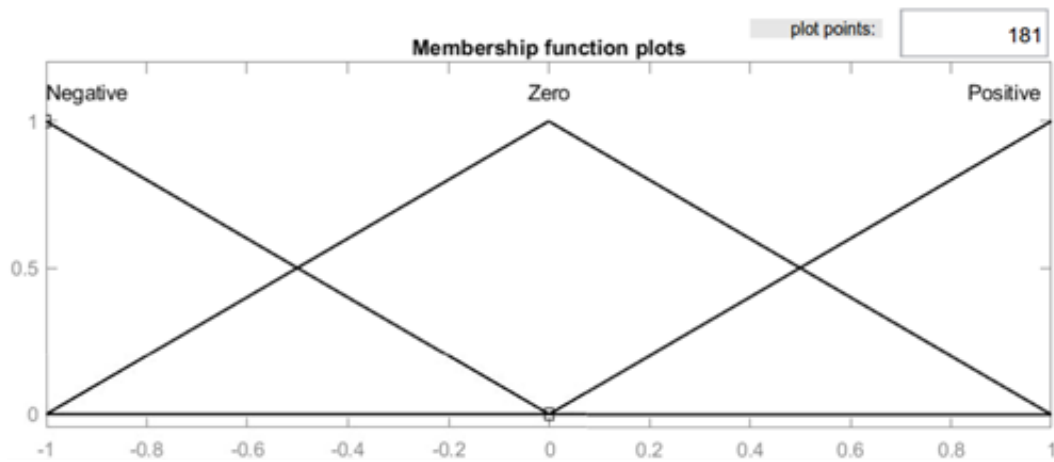
Fig. 6 - FLC input memberships.
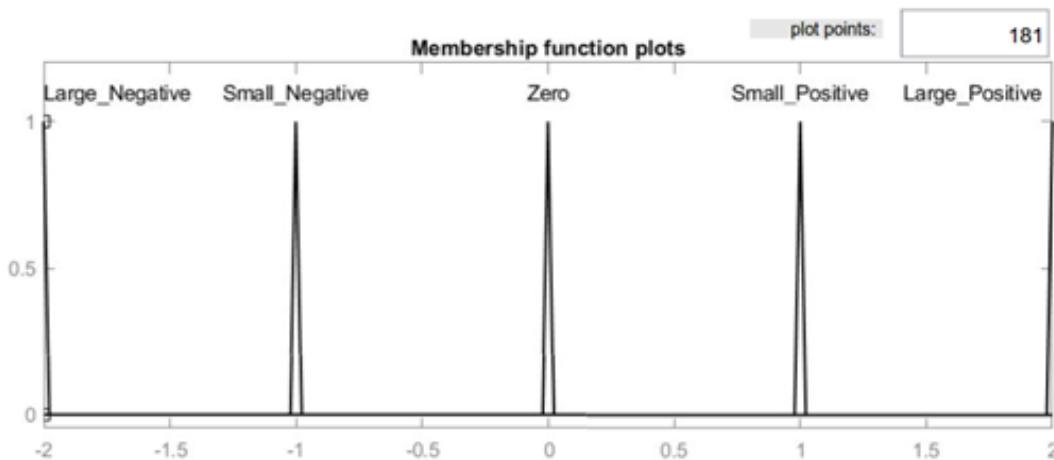
Fig. 7 - FLC output membership.

Table 2 - FLC Rule Base.

Δe e	Negative	Zero	Positive
Negative	Large_Negative	Small_Negative	Zero
Zero	Small_Negative	Zero	Small_Positive
Positive	Zero	Small Positive	Large_Positive

Table 3 - PID controller gain parameters and FLC gains.

PID Controller Gain Parameters	FLC Gains
Kp	K1*K3+K2*K4
Ki	K1*K4
Kd	K2*K3

Table 4 - PID and F-PID controller gains values.

Parameter	Value
Kp	8.6957
Ki	23.6232
Kd	0.1957
K1	4.045
K2	0.0975
K3	2.0066
K4	5.8329

4. Optimal Fuzzy Based Virtual Inertia Controller

The change in the FLC gains values can change the controller response. Many optimization techniques can be used to find the optimal values depending on random search methods. Particle swarm optimization (PSO) is used with a fuzzy PID controller in [22]. Ant Colony Optimization (ACO) is used in [23] to improve the quality of fuzzy PID controller and work with high performance in many researches [31, 32].

In this section, the optimal values of FLC gains are identified by ant colony optimization (ACO) to obtain the optimal fuzzy PID (OF-PID) controller.

4.1. Ant colony optimization (ACO)

Ant colony optimization (ACO) is a type of meta-heuristic optimization that can handle hard combinatorial optimization problems. It was introduced by Marco Dorigo in 1992[33]. ACO is used to optimize the PID controller parameters for LFC of two interconnected areas [34]. in [35] ACO technique is used to tune a PID controller for frequency regulation of a single area power system. Moreover, ACO is used to define the optimal parameters of PI controller to achieve high performance of Maximum Power Point Tracking of a variable-speed wind turbine [36]. In [33] ACO is used to obtain the optimal parameters of PID controller for single area LFC.

 Ant colony optimization (ACO) was mainly inspired from the ant behavior during looking for food. The ants try to find good food with the shortest route from their colony. During its move, ants deposit pheromones (a chemical material) on the path to guide other ants [23, 37]. The pheromone's density is determined by the quality of the food and the length of the route (the solution). After each ant has created a solution, the pheromone values are updated. This pheromone evaporates over time. Moreover, its quantity grows as the number of ants that follow this path grows. The short route has a higher pheromone density and hence attracts more ants than the long route [38].

To identify the optimal solution, the artificial ants use a series of local motions from a starting location. Each ant in the colony tries to find a solution, and the best solution can be found through the colony's cooperation. The amount of pheromone is updated according to the ACO rules after each tour for the ants. Moreover, the ant dies after finding a solution. The best solution has the maximum quantity of pheromone at the end of each iteration. The ACO rules are used to determine the amount of pheromone deposited or dissipated [31, 39].

Identifying the cost function is the main step to apply ACO, which can achieve the optimal values for the optimal fuzzy PID controller (K1, K2, K3, and K4). OF-PID controller aims to improve the system transient response and enhance its stability. The cost function in eq. 4 provides a time-domain performance specification:

$$f = \frac{1}{(1 - e^{-\beta})(Mp + e_{ss}) + e^{-\beta}(t_s - t_r)} \qquad (4)$$

Mp: desired maximum overshoot.

ts: desired settling time.

tr: desired rise time.

ess: desired steady-state error.

β: weighting factor.

β is adjusted to a value higher than 0.7 to minimize overshoot and steady-state error or set to less than 0.7 to decrease the rise and settling times [33][40]. To obtain the optimal values, β is set to 0.7.

The ACO algorithm is applied in this research to optimize the tuning of OF-PID parameters K1, K2, K3, and K4 by minimizing the required cost function. The range of these parameters is identified from the stability point of view, taking into consideration the parameter values in the F-PID controller:

$$K1^{min} \leq K1 \leq K1^{max}$$
$$K2^{min} \leq K2 \leq K2^{max}$$
$$K3^{min} \leq K3 \leq K3^{max}$$
$$K4^{min} \leq K4 \leq K4^{max}$$

Fig. 8 shows the flowchart for this optimization procedure. The ending procedure of the algorithm is dependent on the maximum number of iterations. When it is reached, the algorithm will end. The optimal gain values for the OF-PID controller are shown in Table 5. ACO improves the quality of the fuzzy PID controller, which improves the studied islanded microgrid dynamic response with high penetration of RESs.
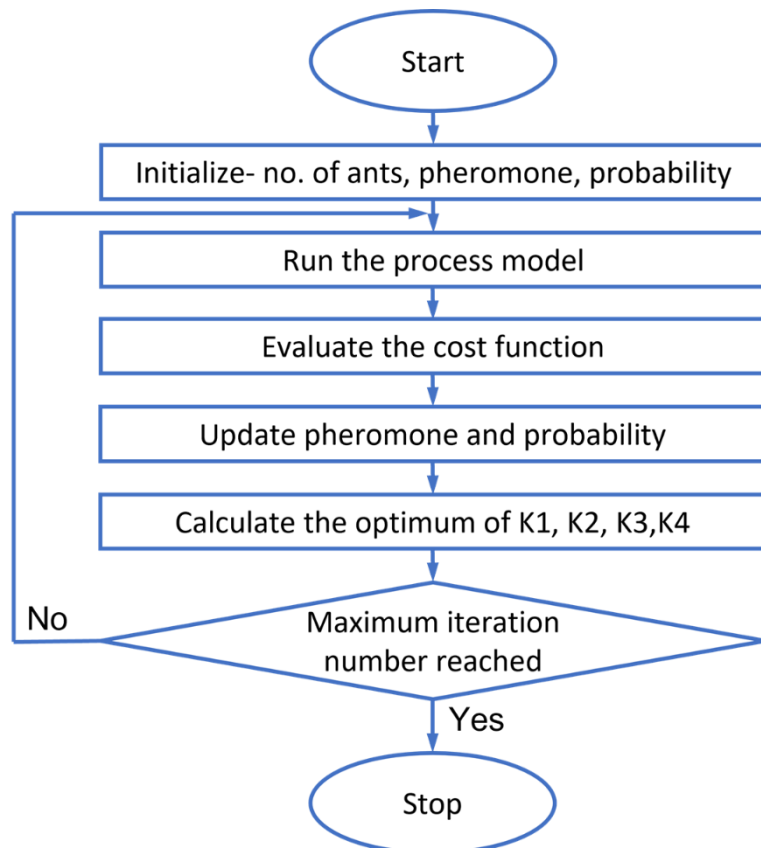
Fig. 8 - Flowchart of Ant colony optimization based OF-PID controller.

Table 5 - optimal gains values for the OF-PID controller.

Parameter	Value
K1	5.26
K2	2.435
K3	0.3007
K4	18

5. Virtual Inertia Control Based on Relative Rate Observer (RRO) Self-Tuning Fuzzy PID (RROSTF-PID)

Relative Rate Observer Self-Tuning Fuzzy PID (RROSTF-PID) adds online tuning of integral and derivative coefficients for the optimal fuzzy PID controller. This advantage makes the controller more flexible and improves the system response. That tuning depended on the state of the system. This method adjusts the two coefficients depending on using a fuzzy inference mechanism in an online technique. System error (e) and the additional variable rv ''normalized acceleration'' in [41] are the two inputs of the fuzzy inference mechanism that sets integral and derivative coefficients. "Relative rate" information about the system response (fastness-slowness) is given by the normalized acceleration rv(i), which is defined as [42, 43]:

$$r_v(k) = \frac{de\,(i) - de\,(i-1)}{de\,(.)} = \frac{dde\,(i)}{de\,(.)} \tag{5}$$

Here, de (i): the incremental change in error and it is given by

$$de\,(i) = e\,(i) - e\,(i-1) \tag{6}$$

and dde (k): the acceleration in error and it is given by

$$dde\,(i) = de\,(i) - de\,(i-1) \tag{7}$$

In [44], de (.) is chosen as follows:

$$de\,(.) = \begin{cases} de\,(i), & if\ |de\,(i)| \geq |de\,(i-1)| \\ de\,(i-1), & if\ |de\,(i)| < |de\,(i-1)| \end{cases} \tag{8}$$

Fig. 9 shows the block diagram of the RROSTF-PID controller. ɣ is the output of the fuzzy parameter regulator. The scaling factors k2 and k4 are adjusted as follows:

$$k2 = k_{2s}.\,k_{fd}.\,k_f.\,ɣ \tag{9}$$

$$k4 = \frac{k_{4s}}{k_f.\,ɣ} \tag{10}$$

Fig. 10, shows input memberships, and the output membership is shown in Fig. 11. Table 6 shows the relative rate observer FLC rules, according to [42]. The optimal values of kf and kfd are 0.181 and 2.12 and were obtained here by using ACO.

Table 6 – Relative Rate Observer FLC Rule Base.

rv \ |e|	Slow	Moderate	Fast
Small	Medium	Medium	Large
Small_Medium	Small_Medium	Medium	Large
Medium	Small	Small_Medium	Medium
Large	Small	Small	Small_Medium
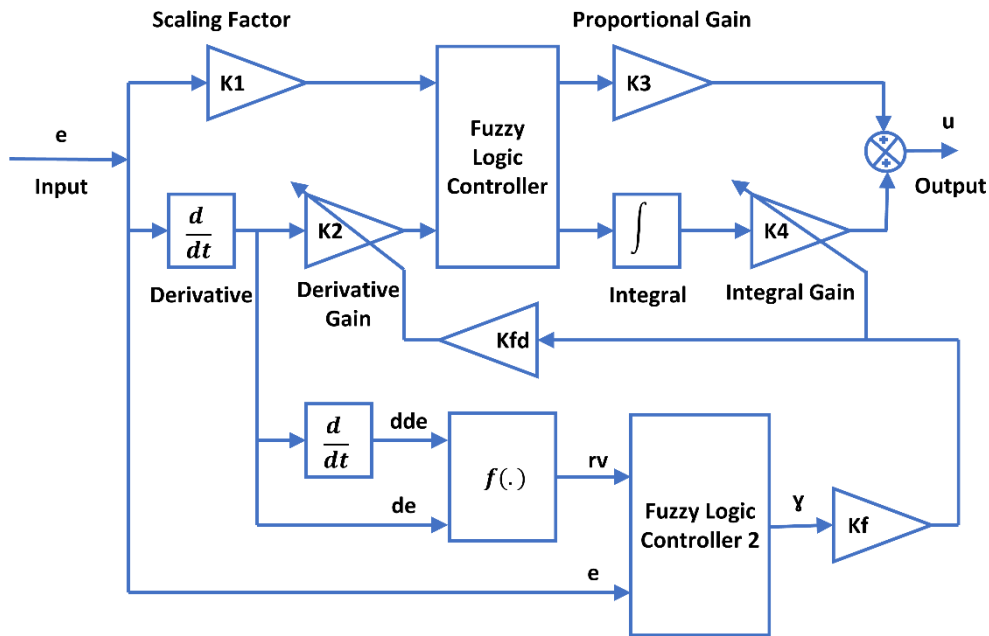
Fig. 9 - the block diagram of the RROSTF-PID controller.

(a)

(b)
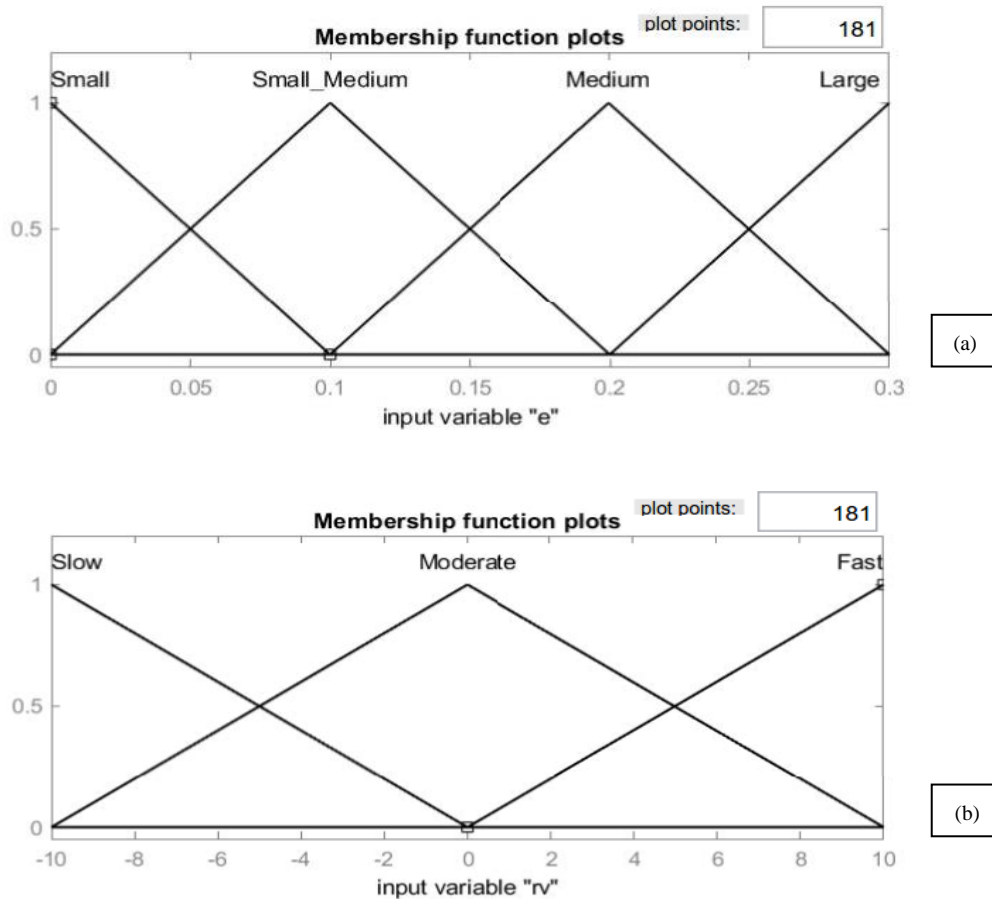
Fig. 10 – RRO FLC input membership: (a) for "e" signal and (b) for "rv" signal.
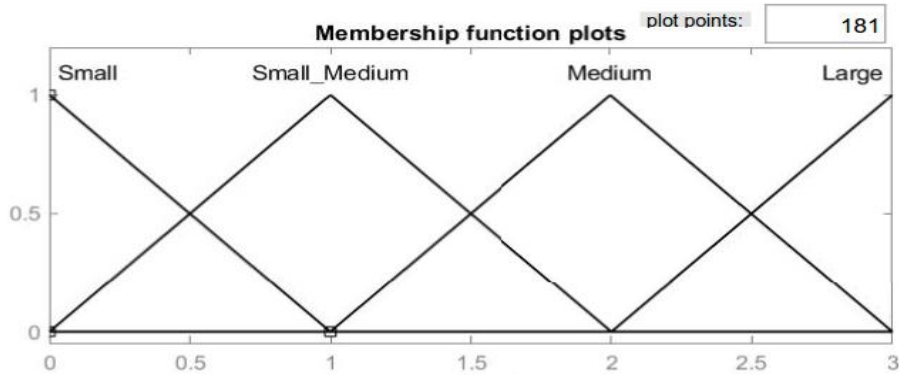
Fig. 11 - RRO FLC output membership.

6. Simulation Results and Analysis

In this section, the performance of the proposed controllers is evaluated by using MATLAB/Simulink under various operating conditions for the studied island microgrid. Furthermore, the effect of a high contribution of RESs is taken into consideration with multiple disturbances and uncertainty conditions. a comparison between the performance of VIC based on RROSTF-PID, VIC based on OF-PID controller, VIC based on F-PID controller, VIC based on optimal PID controller, conventional VIC (CVIC) and the studied island microgrid without VIC is done by using four testing scenarios.

6.1. Various load disturbances

Firstly, load disturbances are applied in scenarios 1 and 2 with a variable value of the studied island microgrid inertia (as uncertainty).

Scenario I: at t=50 sec, 0.1 pu step change in the residential load power has occurred. Moreover, a 0.2 pu step change in the industrial load power occurs at t=100 sec. These disturbances show the frequency variation of the studied island microgrid with full normal system inertia.

As shown in Fig. 12, high fluctuation in the microgrid frequency in the absence of VIC reached ±0.76 Hz at t=100 sec (0.2 pu step change in the industrial load). The CVIC limits the frequency deviation to ±0.64 Hz at t=100 sec. The F-PID-based VIC acts like a PID-based VIC and improves the system stability but with a frequency deviation of ±0.22 Hz at t=100 sec. The frequency deviation was reduced significantly by using OF-PID-based VIC and RROSTF-PID-based VIC. The OF-PID-based VIC enhances the microgrid frequency stability and reduces the frequency deviation to ±0.09 Hz at t=100 sec. The RROSTF-PID-based VIC shows the best performance and has significantly improved the frequency performance. Moreover, it limits the frequency deviation to ±0.04 Hz at t=100 sec. As shown in this scenario, using VIC enhances the microgrid stability and reduces the frequency deviation. Moreover, the flexibility of RROSTF-PID-based VIC due to the online tuning of K2 and K4 makes it perform better than the other controllers.
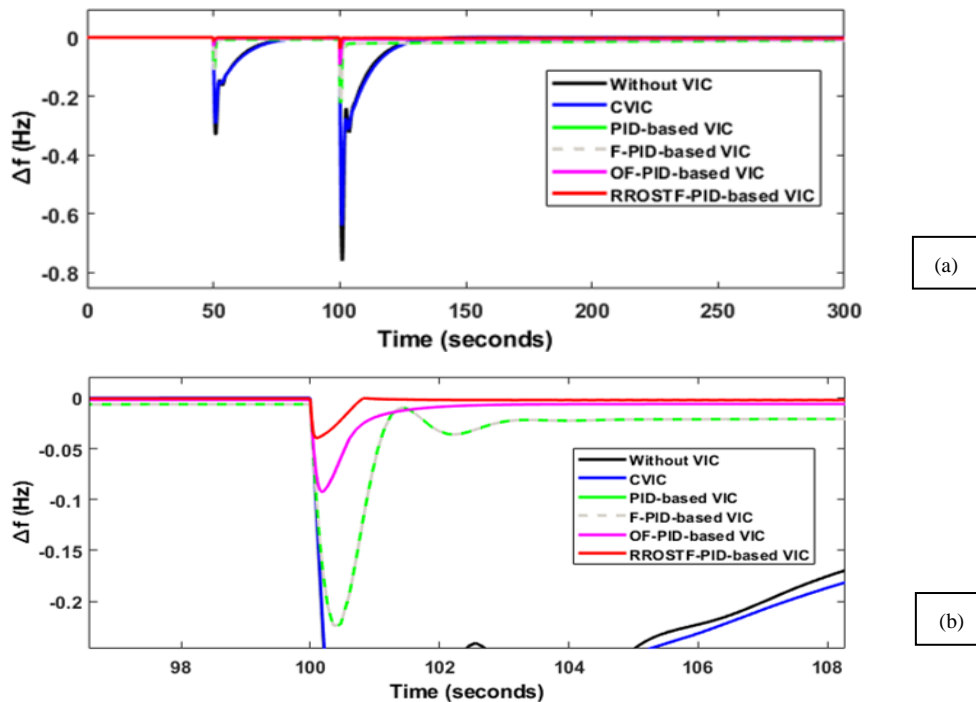
Fig. 12 - Frequency response of the studied islanded microgrid: (a) for scenario I, (b) Comparison between RROSTF-PID, OF-PID, F-PID and PID controller-based VIC in scenario I.

Scenario II: the normal microgrid's inertia is reduced by 40% (as uncertainties). Moreover, the studied islanded microgrid has the same load disturbances as Scenario I.

The reduction in the total microgrid inertia affects the stability of the microgrid. In this case, the microgrid is weak and can't handle some disturbances. That can lead to a blackout. VIC is used to enhance the microgrid stability and prevent a blackout.

Fig. 13, shows the impact of microgrid inertia reduction on the microgrid frequency performance. Without VIC, the microgrid can handle the disturbance at t=50 sec (0.1 pu step change in the residential load) with a frequency deviation reaching ±0.43 Hz, but at t=100 sec (0.2 pu step change in the industrial load), the microgrid loses its stability. While the other controllers based on VIC can save the microgrid stability with different frequency deviations. The frequency deviation reaches ±0.92 Hz at t=100 sec with CVIC and ±0.26 Hz at t=100 sec with PID-based VIC.

The OF-PID-based VIC limits the frequency deviation to ±0.12 Hz at t=100 sec. Moreover, RROSTF-PID-based VIC gives the best performance with the lowest frequency deviation, which does not exceed ±0.06 Hz.
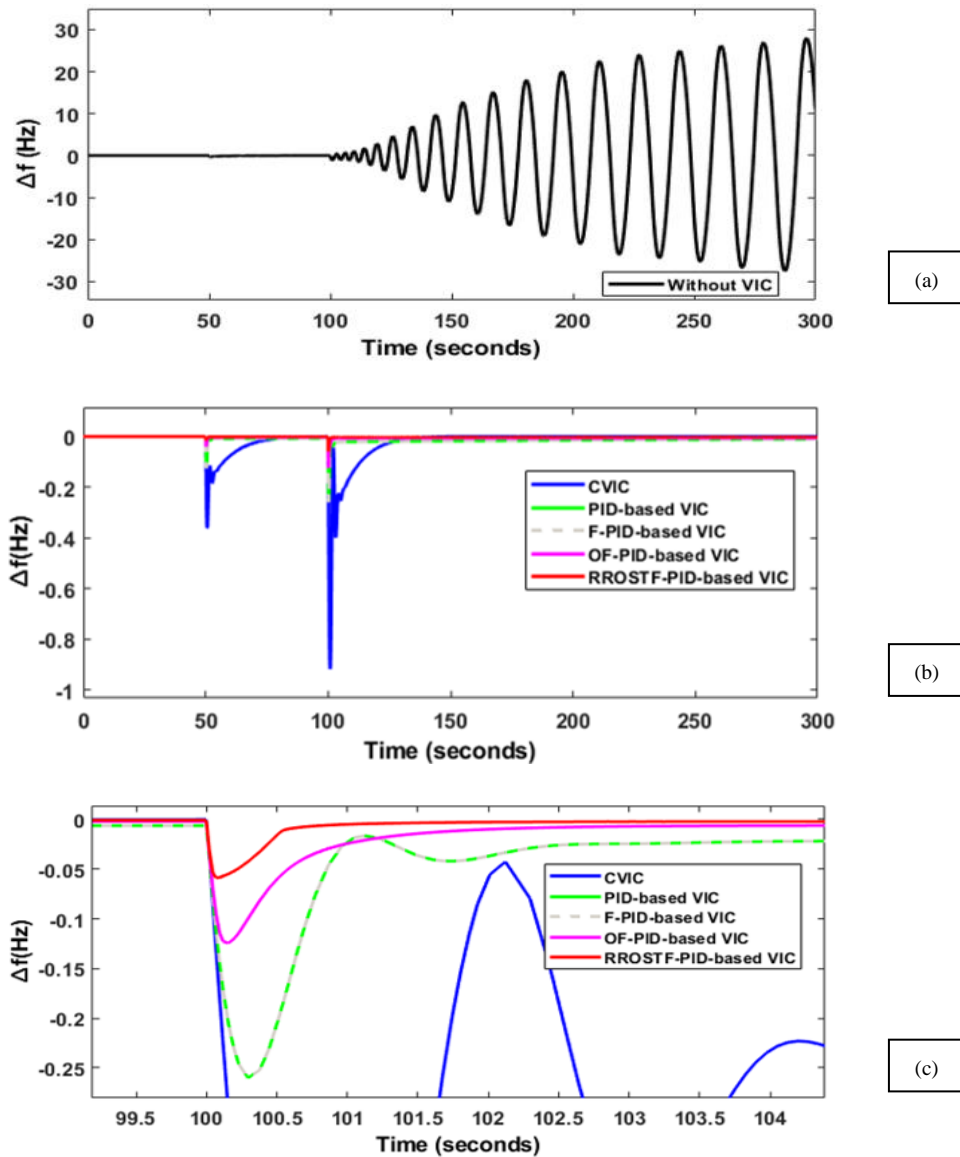
Fig. 13 - Frequency response of the studied islanded microgrid: (a) without VIC in scenario II, (b) for scenario II, (C) Comparison between RROSTF-PID, OF-PID, F-PID and PID controller-based VIC in scenario II.

6.2. *Various Load disturbances and high Penetration of RESs*

Scenarios III and IV show the effect of RESs high contribution to the studied island microgrid. Moreover, these scenarios show the performance of the different proposed controllers with the different load disturbances and the effect of the reduction of the microgrid's inertia (as uncertainties) due to the increase of RESs penetration.

Scenario III: This scenario has different operating conditions as in Table 7. The RESs contribute with high wind power and low solar power. Moreover, this scenario has a high industrial load power step change and a low residential load power step change. Full normal system inertia is used.

The microgrid stability is saved in all cases in this scenario by taking into consideration the high contribution of the RESs. Although there are high-frequency deviations in the microgrid without VIC and with CVIC. As shown in Fig. 14, The microgrid frequency deviations without VIC reach ±0.86 Hz at t=150 sec (0.22 pu step change in industrial load) and reach ±0.73 Hz in the microgrid with CVIC. The microgrid frequency deviations are reduced to ±0.24 Hz at t=150 sec by using PID-based VIC. The frequency performance is improved by using F-PID- based VIC, which limits the frequency deviation to ±0.11 Hz. Moreover, the frequency deviations are minimized and do not exceed ±0.05 Hz when using RROSTF-PID-based VIC. RROSTF-PID-based VIC improves the microgrid stability and its response to different operating conditions. Moreover, it limits the frequency deviations to small values with large disturbances, as shown in this scenario.

Table 7 - microgrid different operation conditions.

Disturbance source	Starting time, sec	Stopping time, sec	Size, pu
solar power plant	initial	-	0.11
wind farm	300 s	-	0.25
residential load	initial	450 s	0.07
industrial load	150 s	-	0.22
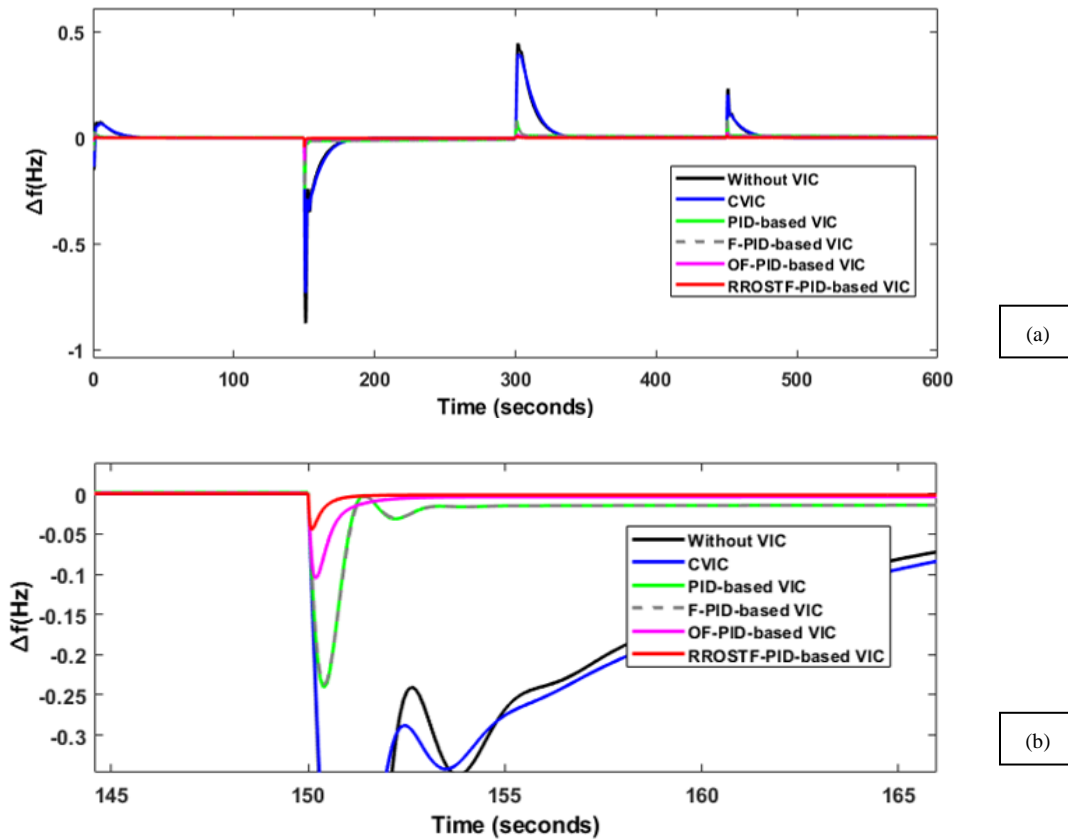
Fig. 14 - Frequency response of the studied islanded microgrid: (a) for scenario III, (b) Comparison between RROSTF-PID, OF-PID, F-PID and PID controller-based VIC in scenario III.

Scenario IV: the same operating conditions as in Scenario III but with an increase in the RESs penetration leading to a decrease of 40% of the microgrid's normal inertia (as uncertainties).

A low inertia microgrid faces many difficulties to save its stability. It may save stability with small disturbances but may lose stability quickly with the change in the operating conditions. As in Fig. 15, the low inertia microgrid without VIC succeeds in saving the stability at t=0 sec (0.11 pu step change in solar power), but after that, the microgrid becomes unstable due to a 0.22 pu step change in the industrial load at t=150 sec. The CVIC enhances the microgrid stability but with a high frequency deviation that reaches ±1 Hz at t=150 sec. PID-based VIC reduces the frequency deviation to ±0.28 Hz. The OF-PID-based VIC limits the frequency deviation to ±0.14 Hz. RROSTF-PID-based VIC prevents a blackout, enhances the microgrid stability, and minimizes frequency deviation to ±0.07 Hz. That allows for more contributions from RESs.
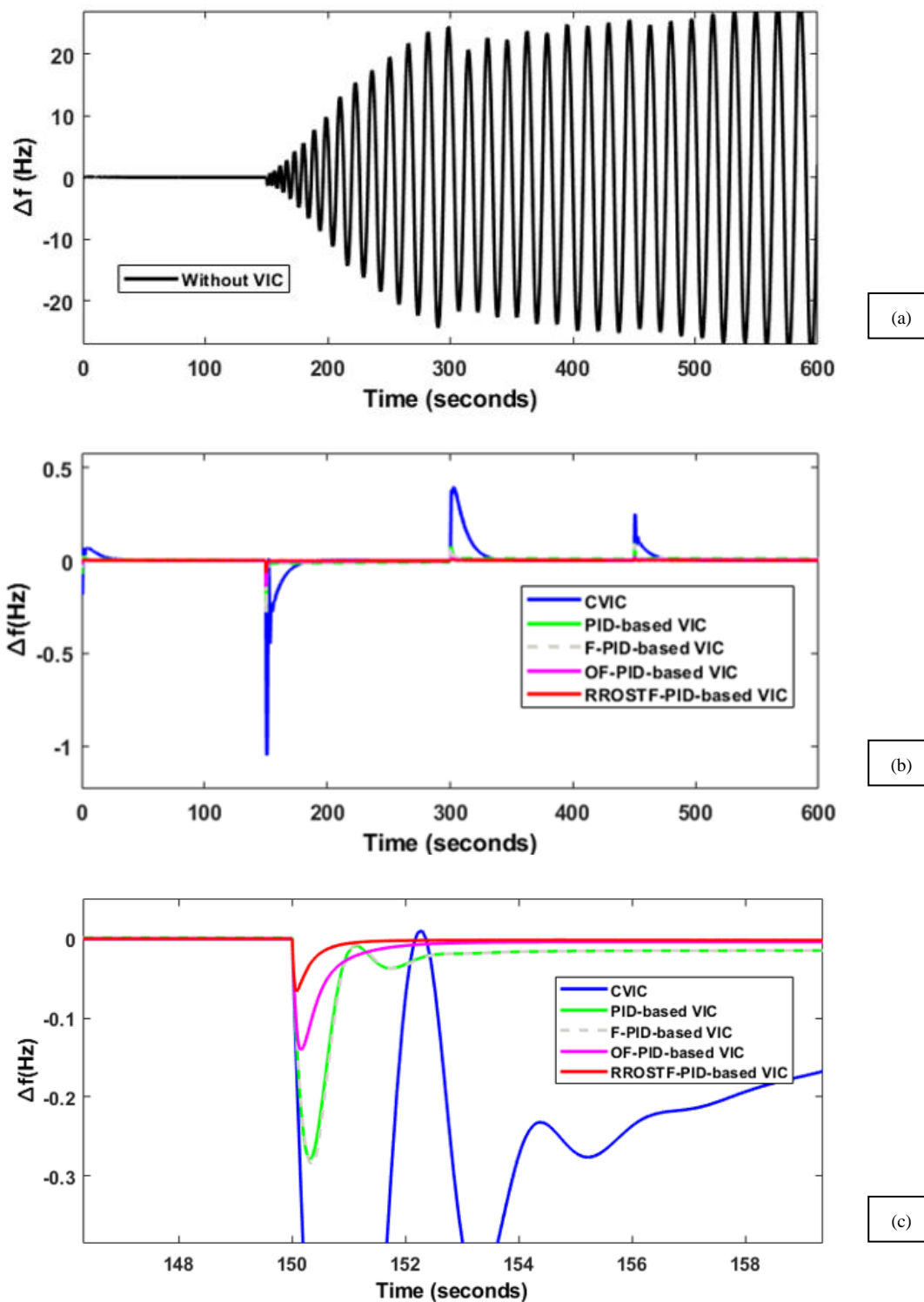
Fig. 15 - Frequency response of the studied islanded microgrid: (a) without VIC in scenario IV, (b) for scenario IV, (C) Comparison between RROSTF-PID, OF-PID, F-PID and PID controller-based VIC in scenario IV.

7. Conclusions

The RESs penetration is increased, and that decreases the system's total inertia. So, saving the stability of the system and improving the frequency performance has become more difficult. The VIC concept is used to handle this issue by simulating the inertia characteristics of traditional generators. VIC depends on calculating the ROCOF to support the system at the contingency conditions.

In this research, RROSTF-PID-based VIC is used to improve the stability and the dynamic response of the studied islanded microgrid. Moreover, it has a low-frequency deviation and can deal with different operating conditions. That allows for an increase in the RESs penetration. Moreover, RROSTF-PID-based VIC proves its efficiency when it is compared with OF-PID-based VIC, F-PID-based VIC, PID-based VIC, and CVIC.

REFERENCES

[1] Magdy, G., Shabib, G., Elbaset, A. A., & Mitani, Y. (2019). Renewable power systems dynamic security using a new coordination of frequency control strategy based on virtual synchronous generator and digital frequency protection. International Journal of Electrical Power & Energy Systems, 109, 351-368.

[2] Kerdphol, T., Rahman, F. S., Watanabe, M., & Mitani, Y. (2019). Robust virtual inertia control of a low inertia microgrid considering frequency measurement effects. IEEE Access, 7, 57550-57560.

[3] Kerdphol, T., Rahman, F. S., Mitani, Y., Watanabe, M., & Küfeoğlu, S. K. (2017). Robust virtual inertia control of an islanded microgrid considering high penetration of renewable energy. IEEE Access, 6, 625-636.

[4] Kerdphol, T., Watanabe, M., Hongesombut, K., & Mitani, Y. (2019). Self-adaptive virtual inertia control-based fuzzy logic to improve frequency stability of microgrid with high renewable penetration. IEEE Access, 7, 76071-76083.

[5] El Zoghby, H. M., & Ramadan, H. S. (2022). Isolated microgrid stability reinforcement using optimally controlled STATCOM. Sustainable Energy Technologies and Assessments, 50, 101883.

[6] Magdy, G., Shabib, G., Elbaset, A. A., & Mitani, Y. (2019). A novel coordination scheme of virtual inertia control and digital protection for microgrid dynamic security considering high renewable energy penetration. IET Renewable Power Generation, 13(3), 462-474.

[7] Kerdphol, T., Rahman, F. S., & Mitani, Y. (2018). Virtual inertia control application to enhance frequency stability of interconnected power systems with high renewable energy penetration. Energies, 11(4), 981.

[8] Fathi, A., Shafiee, Q., & Bevrani, H. (2018). Robust frequency control of microgrids using an extended virtual synchronous generator. IEEE Transactions on Power Systems, 33(6), 6289-6297.

[9] D'Arco, S., Suul, J. A., & Fosso, O. B. (2015). A Virtual Synchronous Machine implementation for distributed control of power converters in SmartGrids. Electric Power Systems Research, 122, 180-197.

[10] Yap, K. Y., Lim, J. M. Y., & Sarimuthu, C. R. (2021). A novel adaptive virtual inertia control strategy under varying irradiance and temperature in grid-connected solar power system. International Journal of Electrical Power & Energy Systems, 132, 107180.

[11] Zhang, L., Wang, X., Zhang, Z., Cui, Y., Ling, L., & Cai, G. (2022). An adaptative control strategy for interfacing converter of hybrid microgrid based on improved virtual synchronous generator. IET Renewable Power Generation, 16(2), 261-273.

[12] Xing, W., Wang, H., Lu, L., Han, X., Sun, K., & Ouyang, M. (2021). An adaptive virtual inertia control strategy for distributed battery energy storage system in microgrids. Energy, 233, 121155.

[13] Singh, K. (2021). Enhancement of frequency regulation in tidal turbine power plant using virtual inertia from capacitive energy storage system. Journal of Energy Storage, 35, 102332.

[14] Kerdphol, T., Watanabe, M., Mitani, Y., & Phunpeng, V. (2019). Applying virtual inertia control topology to SMES system for frequency stability improvement of low-inertia microgrids driven by high renewables. Energies, 12(20), 3902.

[15] Li, D., Zhu, Q., Lin, S., & Bian, X. Y. (2016). A self-adaptive inertia and damping combination control of VSG to support frequency stability. IEEE Transactions on Energy Conversion, 32(1), 397-398.

[16] Said, S. M., Aly, M., Hartmann, B., & Mohamed, E. A. (2021). Coordinated fuzzy logic-based virtual inertia controller and frequency relay scheme for reliable operation of low-inertia power system. IET Renewable Power Generation, 15(6), 1286-1300.

[17] Bevrani, H., Ise, T., & Miura, Y. (2014). Virtual synchronous generators: A survey and new perspectives. International Journal of Electrical Power & Energy Systems, 54, 244-254.

[18] Zadeh, L. A. (1973). Outline of a new approach to the analysis of complex systems and decision processes. IEEE Transactions on systems, Man, and Cybernetics, (1), 28-44.

[19] Mamdani, E. H. (1974). Applications of fuzzy algorithms for simple dynamic plant. Porc. IEE. vol. 121, n. 12, pp. 1585-1588.

[20] Li, H. X., Zhang, L., Cai, K. Y., & Chen, G. (2005). An improved robust fuzzy-PID controller with optimal fuzzy reasoning. IEEE Transactions on Systems, Man, and Cybernetics, Part B (Cybernetics), 35(6), 1283-1294.

[21] Li, H. X., & Gatland, H. (1996). Conventional fuzzy control and its enhancement. IEEE Transactions on Systems, Man, and Cybernetics, Part B (Cybernetics), 26(5), 791-797.

[22] Eltag, K., Aslamx, M. S., & Ullah, R. (2019). Dynamic stability enhancement using fuzzy PID control technology for power system. International Journal of Control, Automation and Systems, 17(1), 234-242.

[23] Chen, G., Li, Z., Zhang, Z., & Li, S. (2019). An improved ACO algorithm optimized fuzzy PID controller for load frequency control in multi area

interconnected power systems. IEEE Access, 8, 6429-6447.

[24] RM Kuraz, Y., & MF Algreer, M. (2008). Design fuzzy self tuning of PID controller for chopper-fed DC motor drive. Al-Rafidain Engineering Journal (AREJ), 16(2), 54-66.

[25] Anantwar, H., Lakshmikantha, B. R., & Sundar, S. (2017). Fuzzy self tuning PI controller based inverter control for voltage regulation in off-grid hybrid power system. Energy Procedia, 117, 409-416.

[26] Ghany, A., Bahgat, M. E., Refaey, W. M., & Hassan, F. N. (2014, May). Design of Fuzzy PID Load Frequency Controller Tuned by Relative Rate Observer for the Egyptian Power System. In The International Conference on Electrical Engineering (Vol. 9, No. 9th International Conference on Electrical Engineering ICEENG 2014, pp. 1-22). Military Technical College.

[27] Lal, D. K., Barisal, A. K., & Tripathy, M. (2018, February). Load frequency control of multi area interconnected microgrid power system using grasshopper optimization algorithm optimized fuzzy PID controller. In 2018 Recent Advances on Engineering, Technology and Computational Sciences (RAETCS) (pp. 1-6). IEEE.

[28] Chen, G. (1996). Conventional and fuzzy PID controllers: An overview. International Journal of Intelligent and Control Systems, 1(2), 235-246.

[29] Mann, G. K. I., Hu, B. G., & Gosine, R. G. (1997, May). Fuzzy PID controller structures. In CCECE'97. Canadian Conference on Electrical and Computer Engineering. Engineering Innovation: Voyage of Discovery. Conference Proceedings (Vol. 2, pp. 788-791). IEEE.

[30] Mann, G. K. I., Hu, B. G., & Gosine, R. G. (1997, July). Analysis and performance evaluation of linear-like fuzzy PI and PID controllers. In Proceedings of 6th International Fuzzy Systems Conference (Vol. 1, pp. 383-390). IEEE.

[31] Chiha, I., Liouane, N., & Borne, P. (2012). Tuning PID controller using multiobjective ant colony optimization. Applied Computational Intelligence and Soft Computing, 2012.

[32] Ahmad, A., Kashif, S. A. R., Nasir, A., Rasool, A., Liaquat, S., Padmanaban, S., & Mihet-Popa, L. (2021). Controller parameters optimization for multi-terminal DC power system using ant colony optimization. IEEE Access, 9, 59910-59919.

[33] Omar, M., Soliman, M., Ghany, A. A., & Bendary, F. (2013, August). Ant Colony Optimization based PID for single area load frequency control. In 2013 5th International Conference on Modelling, Identification and Control (ICMIC) (pp. 119-123). IEEE.

[34] Nguyen, G. N., Jagatheesan, K., Ashour, A. S., Anand, B., & Dey, N. (2018). Ant colony optimization based load frequency control of multi-area interconnected thermal power system with governor dead-band nonlinearity. In Smart trends in systems, Security and Sustainability (pp. 157-167). Springer, Singapore.

[35] Dhanasekaran, B., Siddhan, S., & Kaliannan, J. (2020). Ant colony optimization technique tuned controller for frequency regulation of single area nuclear power generating system. Microprocessors and Microsystems, 73, 102953.

[36] Mokhtari, Y., & Rekioua, D. (2018). High performance of maximum power point tracking using ant colony algorithm in wind turbine. Renewable energy, 126, 1055-1063.

[37] Ghany, M. A., & Shamseldin, M. A. (2020). Parallel distribution compensation PID based on Takagi-Sugeno fuzzy model applied on Egyptian load frequency control. International Journal of Electrical and Computer Engineering, 10(5), 5274.

[38] M. Dorigo, and Th. Stu "Ant Colony Optimization", tzle.p. cm."A. Bradford book". Includes bibliographical references (p.).ISBN 0-262-04219-3 (alk. paper).

[39] Bhateshvar, Y. K., Mathur, H. D., Siguerdidjane, H., & Bansal, R. C. (2017). Ant colony optimized fuzzy control solution for frequency oscillation suppression. Electric Power Components and Systems, 45(14), 1573-1584.

[40] Shamseldin, M., Abdel Ghany, M., & Hendawey, Y. (2021). Optimal Nonlinear PID Speed Control Based on Harmony Search for An Electric Vehicle. Future Engineering Journal, 2(1), 4.

[41] Güzelkaya, M., & Gürleyen, F. (2001). A new methodology for designing a fuzzy logic controller and PI, PD blending mechanism. Journal of Intelligent & Fuzzy Systems, 11(1-2), 85-98.

[42] Karasakal, O., Yeşil, E., Güzelkaya, M., & Eksin, İ. (2005). Implementation of a new self-tuning fuzzy PID controller on PLC. Turkish Journal of Electrical Engineering and Computer Sciences, 13(2), 277-286.

[43] Güzelkaya, M., Eksin, I., & Yeşil, E. (2003). Self-tuning of PID-type fuzzy logic controller coefficients via relative rate observer. Engineering applications of artificial intelligence, 16(3), 227-236.

[44] He, S. Z., Tan, S., Xu, F. L., & Wang, P. Z. (1993). Fuzzy self-tuning of PID controllers. Fuzzy sets and systems, 56(1), 37-46.